ELSEVIER

Development of a safe neutralization assay for SARS-CoV and characterization of S-glycoprotein

Dong P. Han,[a] Hyung G. Kim,[a] Young B. Kim,[a,1] Leo L.M. Poon,[b] and Michael W. Cho[a,*]

[a] Department of Medicine, Case Western Reserve University School of Medicine, Cleveland, OH 44106, USA
[b] Department of Microbiology, Queen Mary Hospital, University of Hong Kong, Hong Kong, China

Abstract

The etiological agent of severe acute respiratory syndrome (SARS) has been identified as a novel coronavirus SARS-CoV. Similar to other coronaviruses, spike (S)-glycoprotein of the virus interacts with a cellular receptor and mediates membrane fusion to allow viral entry into susceptible target cells. Accordingly, S-protein plays an important role in virus infection cycle and is the primary target of neutralizing antibodies. To begin to understand its biochemical and immunological properties, we expressed both full-length and ectodomain of the protein in various primate cells. Our results show that the protein has an electrophoretic mobility of about 160–170 kDa. The protein is glycosylated with high mannose and/or hybrid oligosaccharides, which account for approximately 30 kDa of the apparent protein mass. The detection of S-protein by immunoassays was difficult using human convalescent sera, suggesting that the protein may not elicit strong humoral immune response in virus-infected patients. We were able to pseudotype murine leukemia virus particles with S-protein and produce SARS pseudoviruses. Pseudoviruses infected Vero E6 cells in a pH-independent manner and the infection could be specifically inhibited by convalescent sera. Consistent with low levels of antibodies against S-protein, neutralizing activity was weak with 50% neutralization titers ranging between 1:15 to 1:25. To facilitate quantifying pseudovirus-infected cells, which are stained blue with X-Gal, we devised an automated procedure using an ELISPOT analyzer. The high-throughput capacity of this procedure and the safety of using SARS pseudoviruses should make possible large-scale analyses of neutralizing antibody responses against SARS-CoV.
© 2004 Elsevier Inc. All rights reserved.

Keywords: SARS; Neutralization assay; Pseudovirus; Glycosylation; Coronavirus; S-protein

Introduction

During the first epidemic of severe acute respiratory syndrome (SARS), which began in November of 2002 in Guandong Province of the People's Republic of China, and lasted for about 7 months, close to 8100 people were infected worldwide, among which 774 people died (WHO, 2003). The etiological agent of this atypical respiratory disease has been identified as a novel coronavirus (designated as SARS-CoV) (Drosten et al., 2003; Fouchier et al., 2003; Ksiazek et al., 2003; Peiris et al., 2003; Poutanen et al., 2003). With a mortality rate of over 9%, SARS-CoV had a major health and socioeconomic impact. Fortunately, there have been very few incidences of SARS infections during the winter season of 2003–2004. However, with multiple modes of virus transmission and a wide range of potential nonhuman reservoirs including wild animals commonly found in markets (e.g., civet cats and raccoon dogs; Guan et al., 2003) as well as domestic cats (Martina et al., 2003), it is highly likely that a virus of this nature will most certainly resurface in the future. Currently, there are no antiviral drugs, immunotherapeutic agents, or vaccines available against the virus. To better control or prevent future epidemics, anti-SARS-CoV drugs and/or vaccines need to be developed.

SARS-CoV belongs to Coronaviridae family. The genomic organization of the virus is similar to that of other coronaviruses with a general order of replicase (Rep; ORFs-1a and 1b), spike (S)-glycoprotein, envelope (E), membrane

* Corresponding author. Department of Medicine, Division of Infectious Diseases, Case Western Reserve University School of Medicine, 10900 Euclid Avenue, Cleveland, OH 44106-4984. Fax: +1-216-844-1409.
E-mail address: mcho@case.edu (M.W. Cho).
[1] Current address: Department of Animal Biotechnology, Konkuk University, Hwayang-dong, Kwangjin-gu, Seoul 143-701, South Korea.

protein (M), and nucleocapsid (N) from 5′ to 3′ direction (Marra et al., 2003; Rota et al., 2003) (Fig. 1). Several open-reading frames have also been identified, which may encode additional proteins (Marra et al., 2003; Rota et al., 2003; Snijder et al., 2003). Their functions, however, are not known at the present time. The protein of a major interest as a target of antiviral drug development efforts as well as for developing vaccines is S-glycoprotein. S-protein of coronaviruses, which is thought to function as a trimer (Delmas and Laude, 1990), is responsible for both binding to cellular receptors and inducing membrane fusion for virus entry into target cells (Collins et al., 1982; Godet et al., 1994; Kubo et al., 1994). Mutations in the protein have been shown to alter virulence and cellular tropism (Fazakerley et al., 1992; Leparc-Goffart et al., 1998; Sanchez et al., 1999). Taken together, the S-protein plays a critical role in the biology and pathogenesis of coronaviruses. Not surprisingly, it is an important target of virus-neutralizing antibodies (Chang et al., 2002; Collins et al., 1982; Fleming et al., 1983; Godet et al., 1994; Kant et al., 1992; Kubo et al., 1993, 1994; Takase-Yoden et al., 1991). Moreover, mice immunized with a recombinant S-protein, or a peptide derived from it, are protected from lethal challenges with murine hepatitis virus (MHV) (Daniel and Talbot, 1990; Koo et al., 1999).

S-protein is a type I membrane glycoprotein, which is translated on membrane-bound polysomes, inserted into rough endoplasmic reticulum (RER), cotranslationally glycosylated, and transported to the Golgi complex. During the transport, S-proteins are incorporated onto maturing virus particles, which assemble and bud into a compartment that lies between the RER and Golgi (Lai and Holmes, 2001). Virions are carried from Golgi to plasma membrane in secretory vesicles. Virions are released from cells when virion-containing vesicles fuse with plasma membrane. Excess S-proteins not incorporated onto virus particles are transported to the surface of plasma membrane (Lai and Holmes, 2001; Tsai et al., 1999; Yamada et al., 1998). S-protein of SARS-CoV is 1255 amino acids long (Fig. 1). It is predicted to have a 13 amino acid signal peptide at the amino-terminus, a single ectodomain (1182 amino acids) and a transmembrane region followed by a short cytoplasmic tail (28 residues) at the carboxy-terminus (Marra et al., 2003; Rota et al., 2003). Due to low sequence homology between the S-protein of SARS-CoV and that of the other coronaviruses (Marra et al., 2003; Rota et al., 2003), the structural and immunogenic properties of SARS-CoV S-protein must be ascertained experimentally. The cellular receptor for SARS-CoV has recently been identified to be angiotensin-converting enzyme 2 (ACE2; Li et al., 2003). The molecular interactions between the S-protein and ACE2 are not yet known. Better understanding of the interactions could lead to development of virus entry inhibitors.

Neutralizing antibodies (Nabs) play a critical role in protection against a variety of viral diseases. An accurate assessment of Nab responses in virus-infected patients is needed to determine immune correlates of protection. It is also an essential and integral part of a vaccine development process. Conventional virus-neutralization assays require the use of replication-competent, infectious viruses. Evaluating virus-neutralizing activity of a large number of antisera with these assays is undesirable due to safety concerns, especially for a biosafety level 3 (BSL3) pathogen like SARS-CoV. The same safety concerns have prompted our laboratory to utilize replication-defective pseudoviruses for HIV-1 neutralization assay (Kim et al., 2001). In this assay, nonreplicating Moloney murine leukemia virus (MuLV) particles pseudotyped with HIV-1 envelope glycoproteins are used (Schnierle et al., 1997). These pseudoviruses encode a β-galactosidase gene, which allows detection of individual infected cells when stained with X-Gal (5-bromo-4-chloro-3-indolyl-β-D-galactopyranoside). In this study, we report development of a SARS-CoV pseudovirus neutralization assay, which should be particularly valuable for researchers who may not have easy access to BSL3 containment facility. Additionally, we describe a high-throughput system for quantitative analyses of X-Gal stained cells. This assay system should facilitate rapid evaluation of antibody responses to vaccine candidates and/or entry inhibitors against SARS-CoV.

Results

Expression of SARS-CoV S-glycoprotein

To express SARS-CoV S-glycoprotein, we initially cloned a DNA fragment encoding the protein into pcDNA-3 vector (pcDNA-S; Fig. 1B). To detect S-protein, Western blot was performed with convalescent sera from SARS-CoV-infected patients. However, no clear protein band was detected despite number of attempts. We reasoned that one of the possibilities for the inability to detect the protein is a low level of S-protein expressed from pcDNA-S. To increase the amount of S-protein expressed, we subcloned the S gene into pHCMV-G vector (Burns et al., 1993), which expresses high level of vesicular stomatitis virus (VSV) G glycoprotein. Although we were able to express higher amount of S-protein (see below), this was not sufficient to detect a clear band on Western blots. An alternative explanation is that antibodies against the protein in convalescent sera cannot recognize S-protein subjected to denaturing conditions of SDS-PAGE (viz. linear epitopes). However, because results from radioimmunoprecipitation and indirect immunofluorescence assays were also ambiguous, it is most likely that the antibody titer against S-protein is very low in convalescent sera.

To further increase protein expression level, S gene was subcloned into a pTM vector (Moss et al., 1990). With this vector, a protein of interest is under the control of a strong T7 RNA polymerase (T7RNAP) promoter and the protein is expressed when cells transfected with the plasmid are
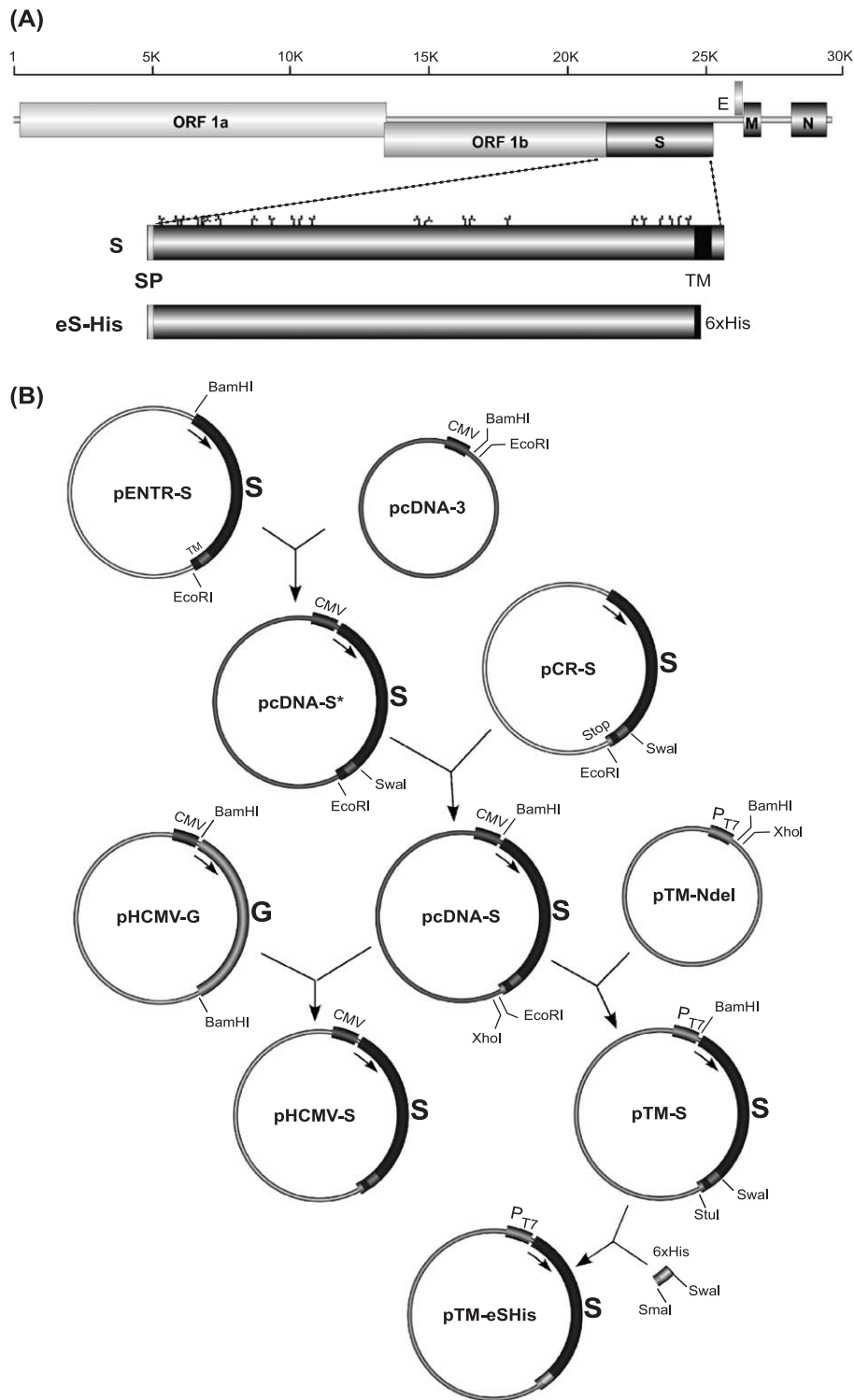
Fig. 1. Construction of SARS-CoV S glycoprotein expression vectors. (A) Genomic organization of SARS-CoV. Only the major nonstructural (replicase ORF1a and 1b) and structural genes (S, E, M, and N) are illustrated. The signal peptide (SP) and transmembrane (TM) domains of the S-protein, and the locations of 23 potential N-linked glycosylation sites, are indicated. Histidine-tagged ectodomain of S-protein is indicated as eS-His. (B) A cloning strategy for expressing S glycoprotein. See Materials and methods for details.

infected with a recombinant vaccinia virus expressing T7RNAP (vTF7-3; Fuerst et al., 1986). The presence of encephalomyocarditis virus Internal Ribosome Entry Site (IRES) at the 5′ end of RNA transcripts allows efficient translation of mRNA transcribed in cytoplasm. Using pTM-S, we were able to detect a faint, but distinct band of approximately 160–170 kDa by Western blot (Fig. 2A, lane 3). We also reevaluated pcDNA-S as this vector has a dual promoter system (CMV and T7 promoter). Using T7 promoter, we were able to detect a protein band of a similar size, albeit less clear than using pTM-S (lane 2). The lower expression of the protein is likely due to the lack of IRES in the pcDNA vector.

Because the calculated molecular weight of S-protein without 13 amino acid signal peptide is about 138 kDa, the result suggested posttranslational modification (e.g., glycosylation). To better demonstrate this, we generated another clone (pTM-eSHis) that expresses the entire ectodomain of S-protein (amino acids 1–1190) with a six-histidine tag at the carboxy terminus. The ectodomain of S-protein migrated with an approximate molecular weight of 163 kDa while its calculated molecular weight is only 131.2 kDa (Fig. 2B, lane 2). To demonstrate that this difference is due to glycosylation, eSHis protein was treated with endoglycosidase H (Endo-H) or peptide: N-glycosidase F (PNGase F). As shown in Fig. 2B (lanes 3 and 4), treatment with either glycosidase increased the mobility of the protein to approximately 133 kDa. Because the mobility of the protein treated with either glycosidases was the same, S-protein is most likely modified with high mannose and/or hybrid, rather than complex, oligosaccharides. While S-glycoprotein of
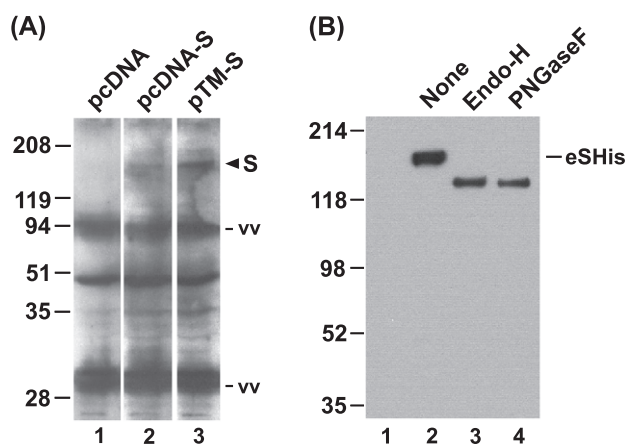

Fig. 2. Analyses of SARS-CoV S-protein glycosylation. (A) HeLa cells transfected with either pcDNA (empty vector), pcDNA-S, or pTM-S were infected with vTF7-3. S-protein (triangle) was detected by Western blot using convalescent sera. Vaccinia-virus-specific bands are indicated by VV. Ten percent acrylamide gel was used. (B) Histidine-tagged ectodomain of S-protein expressed in HeLa cells was either untreated (lane 2) or treated with Endo-H or PNGaseF glycosidases (lanes 3 and 4, respectively). The protein was detected by Western blot with anti-6×His antibody. No band was detected from cells transfected with an empty vector (lane 1). Acrylamide gradient gel (4–12%) was used.

some coronaviruses is cleaved into two subdomains, S1 and S2, the fact that we observed only a single band suggests that SARS-CoV S-protein functions as a single unit.

Production and characterization of SARS-CoV pseudoviruses

Despite difficulties in detecting S-protein directly by immunoassays, proteins expressed from both pcDNA-S and pHCMV-S constructs were able to pseudotype MuLV particles to produce SARS pseudoviruses that could readily infect Vero E6 cells (Fig. 3A). None of the other cell lines we tested, including HeLa, A549, 293T, and BS-C-1, were susceptible. This is in contrast to VSV-G pseudotyped viruses, which could infect all cell lines (data not shown). The fact that BS-C-1 cells, which, like Vero E6 cells, are African green monkey kidney cells, were not susceptible was somewhat unexpected. However, when we performed infections with a high multiplicity of infection, we were able to detect infected BS-C-1, albeit at a significantly reduced titer (7–8-fold compared to Vero E6 cells; data not shown). This result was not too surprising because it has been shown that even 293T cells, which express small amounts of ACE2, support some basal level of SARS-CoV replication (Li et al., 2003).

Many pseudovirus-infected cells appeared as a doublet, which is the result of a cell division following integration of MuLV pseudovirus genome encoding β-galactosidase. These doublets are counted as a single infectious unit. A typical yield of SARS pseudoviruses was about 2×10^4 infectious units per milliliter of culture supernatant using pHCMV-S, which was about fivefold greater than using pcDNA-3. This yield is comparable to what we have been able to achieve for HIV-1 pseudoviruses (between 2×10^3 and 2×10^4 depending on envelopes; Kim et al., 2001), but lower than VSV-G pseudovirus yield (between 3×10^4 and 9×10^4 depending on target cell lines used). Interestingly, SARS pseudovirus production was about 20-fold less efficient when plasmid transfection was performed by calcium phosphate method compared with using cationic lipids (lipofection). This difference, however, was not observed for VSV-G pseudovirus production. An additional difference was that a longer incubation time was needed to achieve peak pseudovirus production for SARS-S compared to VSV-G (3 vs. 2 days posttransfection, respectively). The reasons for these discordant results are unknown at the present time.

Cellular entry of coronaviruses can occur either by acidic pH-dependent or -independent pathway (Gallagher et al., 1991; Lai and Holmes, 2001; Li and Cavanagh, 1990, 1992; Nash and Buchmeier, 1997; Payne et al., 1990). To investigate whether SARS-CoV infection requires low pH, we examined sensitivity of pseudovirus infections to lysosomotropic agents chloroquine and NH$_4$Cl. As expected, infectivity of viruses pseudotyped with VSV-G was reduced by chloroquine and NH$_4$Cl in a dose-dependent manner
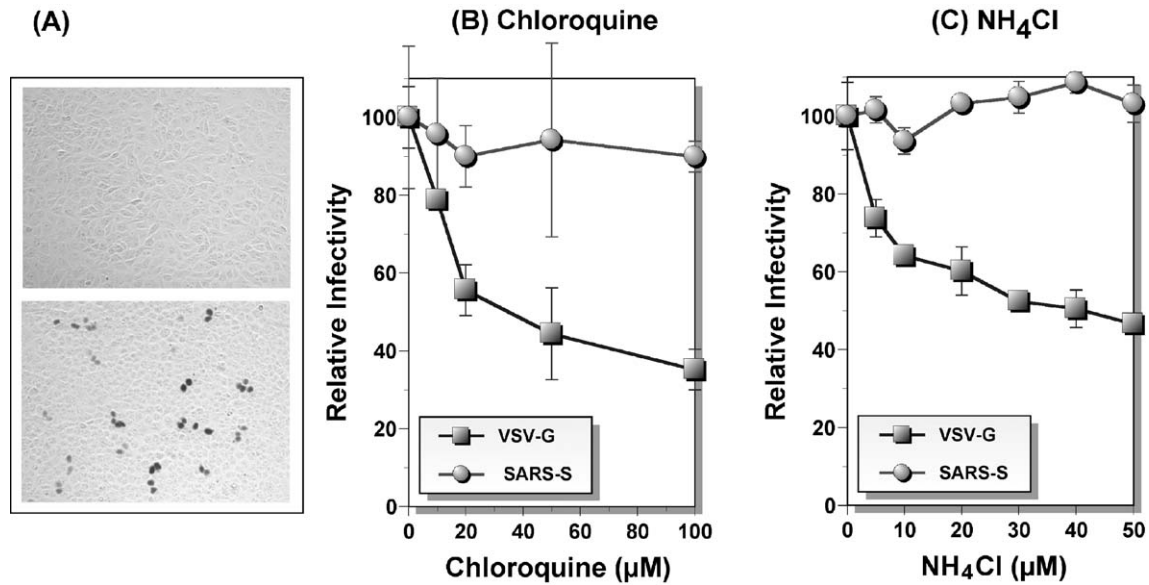
Fig. 3. SARS-CoV pseudovirus infection. (A) Infectivity of SARS pseudoviruses in Vero E6 cells. Infected cells are stained with X-Gal. Mock-infected cells are shown on the top. Infectivity of SARS pseudoviruses was unaffected by lysosomotropic agents chloroquine (B) and by NIH_4Cl (C). In contrast, VSV-G pseudovirus infection was inhibited by both agents.

(Fig. 3B and C, respectively). In contrast, SARS pseudovirus infection was virtually unaffected, suggesting that SARS-CoV infection proceeds in an acidic pH-independent manner.

Neutralization assay

To assess whether SARS pseudoviruses we generated could be used to quantify virus-neutralizing antibodies, we examined their susceptibility to convalescent sera from SARS-CoV-infected patients. As shown in Fig. 4A, sera from two patients were able to specifically neutralize SARS pseudoviruses; the same convalescent sera could not neu-

tralize HIV-1 or VSV-G pseudoviruses and no neutralizing activity was observed with a normal serum. To determine neutralizing antibody titers in virus-infected patients, we performed the assay with serially diluted sera from seven patients. As shown in Fig. 4B, antibody levels were quite similar in all patients with 50% neutralization titer between 1:15 and 1:25.

High-throughput quantification of pseudovirus infections

Although the pseudovirus neutralization assay is sensitive, quantitative, and safe, it has one disadvantage of having to count individual X-Gal-stained cells through a
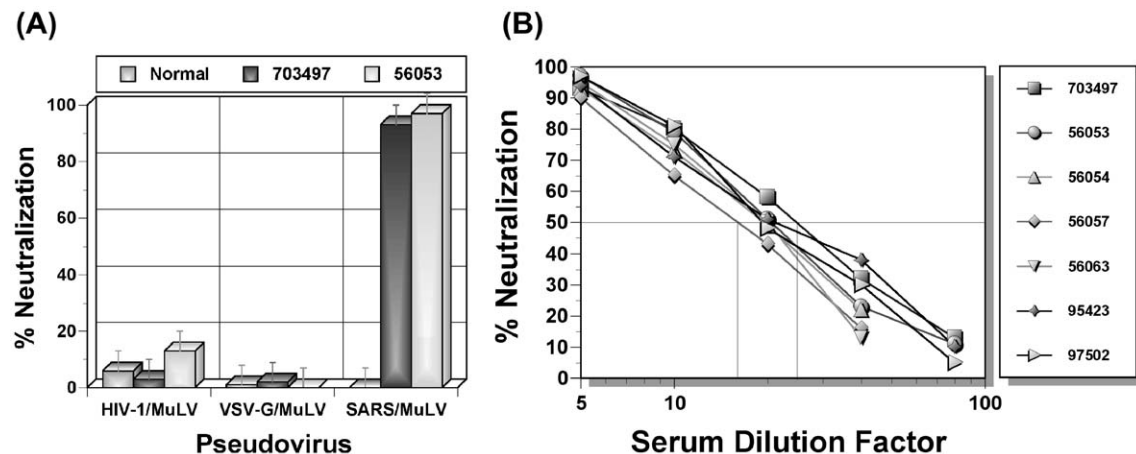

Fig. 4. Pseudovirus neutralization assay. (A) Three different pseudoviruses (HIV 1, VSV-G, and SARS-S) were incubated with either normal serum, or two convalescent sera from patients 703497 and 56053 (1:5 dilution). Neutralizing activity was observed only from convalescent sera from SARS-CoV-infected patients against SARS pseudovirus. HIV-1 pseudovirus infection was done with HOS-CCR5-CD4 cells while VSV-G and SARS-S pseudovirus infections were done with Vero E6 cells. (B) Titration of neutralizing antibodies. Convalescent sera from seven different SARS-CoV patients were used to titer pseudovirus-neutralizing activity. Approximately 70 infectious units were used.
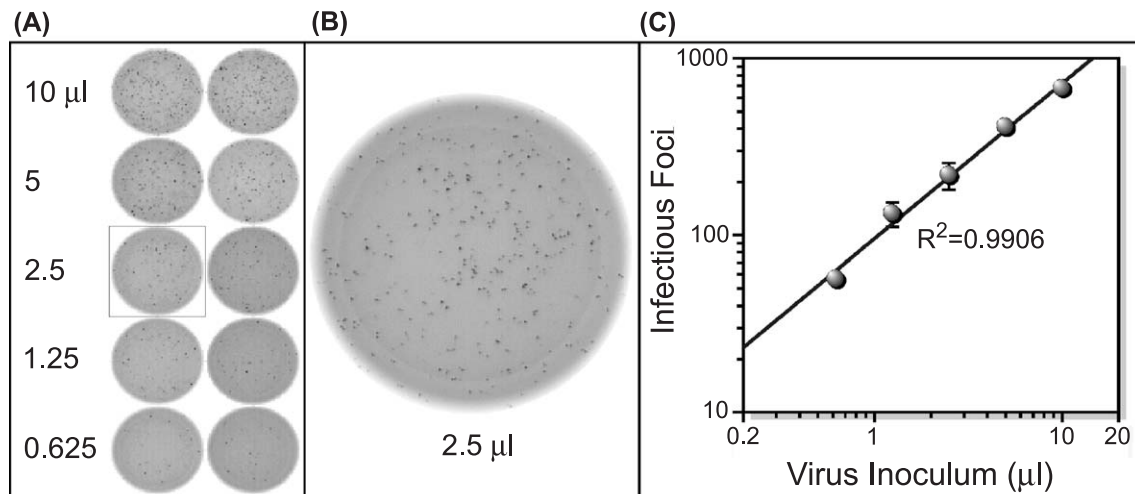
Fig. 5. Automation of counting pseudovirus-infected cells using an ELISPOT reader. HOS cells were infected with twofold serially diluted pseudovirus (10–0.625 μl inoculum) in duplicate, in 96-well plate. MuLV pseudotyped with VSV-G was used. (A) Images of wells infected with five different dilutions of pseudovirus, in duplicate. (B) A magnified image of the boxed well. (C) The number of infectious foci is plotted as a function of virus inoculum.

microscope. To overcome this problem, we looked into a possibility of automating the data collection procedure using an ELISPOT reader (ImmunoSpot Analyzer, Cellular Technology Ltd.). Although this instrument is commonly used to quantify antigen-specific T cell cytokine responses by counting chromogenic immunospots (e.g., IFN-γ), we rationalized that it might be able detect X-Gal-stained blue cells. As shown in Fig. 5, there was no problem with using the instrument to count spots at a single-cell resolution and the analysis was highly efficient as the entire 96-well plate could be processed in less than 20 min. Virus-infected cells appearing as doublets did not pose a problem because parameters on the analysis software could be adjusted to count two stained cells adjacent to each other as one. The number of infectious foci counted was quite linear as a function of virus inoculum (Fig. 5C), validating the methodology. This procedure could be used to quantify other assays based on X-Gal staining of cells (e.g., recombinant vaccinia viruses that express β-galactosidase).

Discussion

In this study, we expressed SARS-CoV S-glycoprotein, which was able to pseudotype MuLV particles. SARS pseudoviruses were able to efficiently infect Vero E6 cells, which have been shown to support SARS-CoV infection. The infection did not require low pH, suggesting viral entry is mediated by a direct fusion event between viral and plasma membranes. This result is consistent with a previous report that cell-to-cell fusion mediated by S-protein and its cellular receptor ACE2 occurred at neutral pH (Xiao et al., 2003). However, our result is in direct disagreement with recently published article by Simmons et al. (2004). There are three major differences in exper-

imental procedures between the two studies. First, we pseudotyped MuLV particles whereas Simmons et al. used HIV-1. Second, we used an authentic S-glycoprotein whereas they used a C-terminal fusion protein that included a V5 epitope and polyhistidine tag, which totaled, by our estimation, 27 extra amino acids. Whether the discrepant result is due to the use of different S-glycoproteins and/or different virus cores needs to be further investigated. The third difference between the studies is the concentrations of lysosomotropic agents used. While we used NH_4Cl at $0–50$ μM amounts, which are sufficient to inhibit VSV-G-mediated fusion (Fig. 3; Picard-Maureau et al., 2003), they used millimolar (mM) amounts. At these concentrations, NH_4Cl could have a secondary effect on S-glycoprotein. We were unable to find concentrations of chloroquine used in their study. It is interesting to note that while Simmons et al. observed that pseudovirus infections required low pH, S-protein-mediated cell-to-cell fusion did not.

The SARS pseudoviruses we generated could be specifically inhibited by convalescent sera from SARS-CoV infected patients, indicating that S-glycoprotein of SARS-CoV is a target of neutralizing antibodies as it is for other coronaviruses. The major purpose of generating SARS pseudoviruses was to devise an assay system to assess virus-neutralizing antibodies safely and rapidly without having to use infectious, replication-competent SARS-CoV. The results of our study indicate that SARS pseudoviruses could be used to evaluate efficacy of various S-glycoprotein-based vaccine candidates to elicit virus-neutralizing antibodies. They could also be used to perform structure–function analyses of S-glycoprotein. Due to a large size of SARS-CoV genome, it would be difficult to perform such analyses directly in the context of the virus, not to mention potential safety hazards from working with it. In contrast,

mutational analyses of the protein could be performed readily using pseudoviruses.

Our attempt to characterize biochemical and immunological properties of the S-protein was hampered by the fact that antibody titers against the protein in convalescent sera were extremely low; we were able to identify only a faint band on a Western blot (with high background) and attempts to detect the protein by immunofluorescence and radio-immunoprecipitation assays were less than successful. In contrast, convalescent sera have been successfully used to detect SARS-CoV-infected cells by an immunofluorescence assay (Hsueh et al., 2003; Peiris et al., 2003). Together, the available data seem to suggest that S-protein might not be immunogenic, at least compared to other viral proteins. In fact, immunoreactivity analyses of a panel of synthetic peptides derived from S, membrane (M), and nucleocapsid (N) proteins suggested that N protein might be the most immunogenic protein (Wang et al., 2003).

The nonimmunogenic nature of S-protein might present potential problems in developing a vaccine that can elicit potent neutralizing antibodies against SARS-CoV. In this regard, it is interesting to note that S-protein is highly glycosylated with 23 potential asparagine-linked glycosylation sites. Based on our analyses of the ectodomain of the protein, carbohydrate residues account for approximately 30 kDa (based on mobility in SDS-PAGE). The glycans were primarily high mannose and/or hybrid type. This, however, needs to be verified using proteins produced from non-vaccinia virus expression system, because the virus infection could possibly affect cellular glycosylation machinery. Extensive glycosylation of HIV-1 envelope glycoprotein has been one of the major obstacles in eliciting good humoral responses against the protein and in developing an effective vaccine against the virus (Cho, 2003). It remains to be seen whether and to what extent glycans on S-protein affect immunogenic properties of the protein. Interestingly, potential glycosylation sites are clustered into three regions of the protein (Fig. 1A): N-terminal, middle, and C-terminal. It has been shown that individual glycosylation sites on HIV-1 surface glycoprotein gp120 may have different functions; while some are important for evading immune responses, others are critical for maintaining proper protein structure necessary to interact with cellular receptors and mediate membrane fusion (Ogert et al., 2001; Reitter et al., 1998). Additional studies are needed to determine whether glycosylation sites in different clusters of S-protein serve different functions.

In the absence of an effective vaccine and/or antiviral drugs against SARS-CoV, early detection of virus-infected patients would be critical for effective containment of future epidemics. Quantitative RT-PCR-based diagnostic assays have been described for SARS-CoV (Grant et al., 2003; Lau et al., 2003; Ng et al., 2003; Poon et al., 2003a, 2003b; Tang et al., 2004; Yam et al., 2003). Despite high sensitivity, their utility has some limitations: (i) the detection rate varies widely between 20% and 80% depending on clinical sam-

ples and protocols used for the assay; (ii) the window of detectability is limited to early stages of infection; and (iii) the assay is not suitable for routine surveillance. Antibodies against SARS proteins have been shown to appear as early as 9 days after the onset of illness (Hsueh et al., 2003). Therefore, development of a high-throughput serology-based diagnostics could complement PCR-based assays. In this regard, a virus-neutralization assay could be used as a confirmatory test, which would enhance the accuracy of early diagnosis of SARS-CoV. Because neutralizing antibodies are important for virus clearance, the assay could also be used to assess disease prognosis. In either case, the availability of SARS pseudoviruses allows avoiding the use of infectious SARS-CoV.

Materials and methods

Construction of S-glycoprotein expression vectors

The overall cloning strategy is shown in Fig. 1B. Two parental plasmids encoding a SARS-CoV S gene (Urbani strain), pENTR-S and pCR-S, were obtained from the U.S. Centers for Disease Control and Prevention. Two S-protein-expressing plasmids (pcDNA-S* and pcDNA-S) were generated using pcDNA-3 (Invitrogen). The S gene in pcDNA-S*, which was transferred from pENTR-S (*Bam*HI−*Eco*RI fragment), lacks the original translation stop codon TAA because it was changed to AAT of *Eco*RI restriction site (gAATtc). pcDNA-S with a stop codon was constructed by replacing a *Swa*I−*Eco*RI fragment of pcDNA-S* with the same fragment from pCR-S. To generate pHCMV-S, a *Bam*HI−*Eco*RI fragment from pcDNA-S was inserted into a *Bam*HI site of pHCMV-G following blunting ends with Klenow. To construct pTM-S, a *Bam*HI−*Xho*I fragment from pcDNA-S was cloned into the corresponding sites of pTM−*Nde*I (Cho et al., 1994). Despite the fact that pTM-S has a small open-reading frame that encodes eight amino acids between the Internal Ribosome Entry Site of pTM-NdeI vector and the S gene, S-protein was efficiently expressed and the plasmid was used as is without further modification. To generate pTM-eSHis, 3′ end of the ecto-domain was PCR amplified using a sense primer 5′-GTC GTC AAC ATT CAA AAA GAA-3′ (nts 3472–3492 of S gene) and an antisense primer 5′-AAT GAA GCG GAT CCCGGG TTA *GTG ATG GTG GTG ATG ATG* **TTG CTC ATA TTT TCC AAA**-3′. Base-pairing region (nts 3553–3570) is shown in bold and the six histidine residues are italicized. The amplified fragment was digested with *Swa*I (nt 3521) and *Sma*I (underlined) and subsequently cloned into pTM-S digested with *Swa*I and *Stu*I.

Cell culture, protein expression, and Western blots

All cell lines, except for Vero E6, were maintained in DMEM supplemented with 10% fetal bovine serum (FBS),

2 mM L-glutamine, and penicillin–streptomycin antibiotics. Vero E6 cells were maintained in EMEM with the same supplements plus 0.1 mM nonessential amino acids. Cells were cultured at 37 °C in 5% CO_2 incubators. To express S-protein, cells were transfected with plasmids by a calcium phosphate precipitation method. Briefly, 0.5 ml of 0.25 M $CaCl_2$ solution containing 30 μg of plasmids was slowly mixed with 2× HBS (50 mM HEPES, 1.5 mM Na_2HPO_4, 280 mM NaCl, pH 7.1) and the mixture was added to cells. After an overnight incubation, culture medium was replaced and cells were further incubated for two additional days. For expression from pTM-S and pTM-eSHis, transfected cells were infected with vTF7-3 (Fuerst et al., 1986) at a multiplicity of infection of 5. Following 2 days of infection, cells were lysed with a hypotonic cell lysis buffer (10 mM Tris, pH 8.0, 10 mM NaCl, 1.5 mM $MgCl_2$, 1% NP-40). Insoluble cell debris and nuclei were removed by a brief centrifugation in a microfuge. Cell lysates were subjected to SDS-PAGE and Western blot. S-proteins were detected with either a pool of convalescent sera (1:100 dilution) or anti-His (C-terminal) monoclonal antibody (Invitrogen; 1:3000 dilution) followed by horseradish peroxidase-conjugated goat anti-human or anti-mouse IgG antibody (Pierce), respectively. Protein bands were visualized using SuperSignal West Pico Chemiluminescence detection system (Pierce). Molecular weights of the protein bands were approximated by the mobility of standard molecular weight markers.

Production of pseudoviruses and infection analyses

Pseudoviruses were generated as previously described (Kim et al., 2001). Briefly, MuLV packaging cell line TELCeB6 (Schnierle et al., 1997) was transfected with pcDNA-S, pHCMV-S, pHCMV-G (Burns et al., 1993), or pLTR-gp140 (HIV-1$_{DH12}$; Kim et al., 2001) using either calcium phosphate precipitation or lipofection (Lipofectin; Invitrogen) method. Two days posttransfection (3 days for SARS pseudovirus), cell culture medium was harvested and subjected to centrifugation ($1700 \times g$, 10 min) to remove cell debris. Supernatant was aliquoted, stored at −80 °C and used as a virus stock.

Virus titer was determined in Vero E6 cells for SARS-S and VSV-G or in HOS-CD4-CCR5 (Cheng-Mayer et al., 1997; Deng et al., 1996) for HIV-1 gp140 pseudotyped viruses. Typically, cells were infected with 60–80 infectious units for 36 h. Cells were washed with PBS and incubated with a fixative (1% formaldehyde, 0.05% glutaraldehyde in PBS) for 10 min at room temperature. The cells were washed twice with PBS and incubated with a freshly prepared staining solution (PBS containing 5 mM potassium ferricyanide, 5 mM potassium ferrocyanide, 2 mM magnesium chloride, and 1 mg/ml of X-Gal) for >2 h at 37 °C. For routine analyses, X-Gal-stained blue cells were manually counted using an inverted microscope.

To determine pH-dependency of viral entry, Vero E6 cells were incubated in culture medium containing 0–100 μM

chloroquine for 1 h at 37 °C before adding viruses. VSV-G or SARS-S pseudoviruses were allowed to adsorb to cells for 1 h at 37 °C in the absence of chloroquine. Following adsorption, virus inoculum was removed, cells were washed, and infection was allowed to proceed for about 36 h in the absence of chloroquine. For NH_4Cl, cells were incubated with 0–50 μM. Due to minimal cytotoxicity, NH_4Cl was present throughout the infection period including 1 h incubation before virus addition. All infections were done in duplicates.

Neutralization assay was performed as previously described (Kim et al., 2001) using convalescent sera (13–50 days post-onset of symptoms) obtained from CDC or from patients hospitalized in Queen Mary Hospital, Hong Kong. Approximately 60–80 infectious units of pseudoviruses were incubated with serially diluted, heat-inactivated (56 °C, 30 min) convalescent or normal sera for 1 h at 37 °C. The mixture was subsequently added to Vero E6 (for SARS-S or VSV-G) or HOS-CD4/CCR5 (for HIV-1 gp140) cells. Virus infection was allowed to proceed for another 36 h. Virus-neutralizing activity was determined relative to no serum control.

Automation of quantifying pseudovirus infection

The general pseudovirus infection procedure is the same as described above. The major difference was that 96-well plates with a white membrane bottom normally used for ELISPOT assays (Plate M200; BD Biosciences) were utilized rather than regular tissue culture plates. ImmunoSpot Analyzer from Cellular Technology Ltd. was used as per manufacturer's recommendations.

References

Burns, J.C., Friedmann, T., Driever, W., Burrascano, M., Yee, J.K., 1993. Vesicular stomatitis virus G glycoprotein pseudotyped retroviral vectors: concentration to very high titer and efficient gene transfer into mammalian and nonmammalian cells. Proc. Natl. Acad. Sci. U. S .A. 90 (17), 8033–8037.

Chang, S.H., Bae, J.L., Kang, T.J., Kim, J., Chung, G.H., Lim, C.W., Laude, H., Yang, M.S., Jang, Y.S., 2002. Identification of the epitope

region capable of inducing neutralizing antibodies against the porcine epidemic diarrhea virus. Mol. Cells 14 (2), 295–299.

Cheng-Mayer, C., Liu, R., Landau, N.R., Stamatatos, L., 1997. Macrophage tropism of human immunodeficiency virus type 1 and utilization of the CC-CKR5 coreceptor. J. Virol. 71 (2), 1657–1661.

Cho, M.W., 2003. Subunit protein vaccines: theoretical and practical considerations for HIV-1. Curr. Mol. Med. 3 (3), 243–263.

Cho, M.W., Teterina, N., Egger, D., Bienz, K., Ehrenfeld, E., 1994. Membrane rearrangement and vesicle induction by recombinant poliovirus 2C and 2BC in human cells. Virology 202 (1), 129–145.

Collins, A.R., Knobler, R.L., Powell, H., Buchmeier, M.J., 1982. Monoclonal antibodies to murine hepatitis virus-4 (strain JHM) define the viral glycoprotein responsible for attachment and cell–cell fusion. Virology 119 (2), 358–371.

Daniel, C., Talbot, P.J., 1990. Protection from lethal coronavirus infection by affinity-purified spike glycoprotein of murine hepatitis virus, strain A59. Virology 174 (1), 87–94.

Delmas, B., Laude, H., 1990. Assembly of coronavirus spike protein into trimers and its role in epitope expression. J. Virol. 64 (11), 5367–5375.

Deng, H., Liu, R., Ellmeier, W., Choe, S., Unutmaz, D., Burkhart, M., Di Marzio, P., Marmon, S., Sutton, R.E., Hill, C.M., Davis, C.B., Peiper, S.C., Schall, T.J., Littman, D.R., Landau, N.R., 1996. Identification of a major co-receptor for primary isolates of HIV-1. Nature 381 (6584), 661–666.

Drosten, C., Gunther, S., Preiser, W., van der Werf, S., Brodt, H.R., Becker, S., Rabenau, H., Panning, M., Kolesnikova, L., Fouchier, R.A., Berger, A., Burguiere, A.M., Cinatl, J., Eickmann, M., Escriou, N., Grywna, K., Kramme, S., Manuguerra, J.C., Muller, S., Rickerts, V., Sturmer, M., Vieth, S., Klenk, H.D., Osterhaus, A.D., Schmitz, H., Doerr, H.W., 2003. Identification of a novel coronavirus in patients with severe acute respiratory syndrome. N. Engl. J. Med. 348 (20), 1967–1976.

Fazakerley, J.K., Parker, S.E., Bloom, F., Buchmeier, M.J., 1992. The V5A13.1 envelope glycoprotein deletion mutant of mouse hepatitis virus type-4 is neuroattenuated by its reduced rate of spread in the central nervous system. Virology 187 (1), 178–188.

Fleming, J.O., Stohlman, S.A., Harmon, R.C., Lai, M.M., Frelinger, J.A., Weiner, L.P., 1983. Antigenic relationships of murine coronaviruses: analysis using monoclonal antibodies to JHM (MHV-4) virus. Virology 131 (2), 296–307.

Fouchier, R.A., Kuiken, T., Schutten, M., Van Amerongen, G., Van Doornum, G.J., Van Den Hoogen, B.G., Peiris, M., Lim, W., Stohr, K., Osterhaus, A.D., 2003. Aetiology: Koch's postulates fulfilled for SARS virus. Nature 423 (6937), 240.

Fuerst, T.R., Niles, E.G., Studier, F.W., Moss, B., 1986. Eukaryotic transient-expression system based on recombinant vaccinia virus that synthesizes bacteriophage T7 RNA polymerase. Proc. Natl. Acad. Sci. U. S .A. 83 (21), 8122–8126.

Gallagher, T.M., Escarmis, C., Buchmeier, M.J., 1991. Alteration of the pH dependence of coronavirus-induced cell fusion: effect of mutations in the spike glycoprotein. J. Virol. 65 (4), 1916–1928.

Godet, M., Grosclaude, J., Delmas, B., Laude, H., 1994. Major receptor-binding and neutralization determinants are located within the same domain of the transmissible gastroenteritis virus (coronavirus) spike protein. J. Virol. 68 (12), 8008–8016.

Grant, P.R., Garson, J.A., Tedder, R.S., Chan, P.K., Tam, J.S., Sung, J.J., 2003. Detection of SARS coronavirus in plasma by real-time RT-PCR. N. Engl. J. Med. 349 (25), 2468–2469.

Guan, Y., Zheng, B.J., He, Y.Q., Liu, X.L., Zhuang, Z.X., Cheung, C.L., Luo, S.W., Li, P.H., Zhang, L.J., Guan, Y.J., Butt, K.M., Wong, K.L., Chan, K.W., Lim, W., Shortridge, K.F., Yuen, K.Y., Peiris, J.S., Poon, L.L., 2003. Isolation and characterization of viruses related to the SARS coronavirus from animals in southern China. Science 302 (5643), 276–278.

Hsueh, P.R., Hsiao, C.H., Yeh, S.H., Wang, W.K., Chen, P.J., Wang, J.T., Chang, S.C., Kao, C.L., Yang, P.C., 2003. Microbiologic characteristics, serologic responses, and clinical manifestations in severe acute respiratory syndrome, Taiwan. Emerg. Infect. Dis. 9 (9), 1163–1167.

Kant, A., Koch, G., van Roozelaar, D.J., Kusters, J.G., Poelwijk, F.A., van der Zeijst, B.A., 1992. Location of antigenic sites defined by neutralizing monoclonal antibodies on the S1 avian infectious bronchitis virus glycopolypeptide. J. Gen. Virol. 73 (Pt 3), 591–596.

Kim, Y.B., Lee, M.K., Han, D.P., Cho, M.W., 2001. Development of a safe and rapid neutralization assay using murine leukemia virus pseudotyped with HIV type 1 envelope glycoprotein lacking the cytoplasmic domain. AIDS Res. Hum. Retroviruses 17 (18), 1715–1724.

Koo, M., Bendahmane, M., Lettieri, G.A., Paoletti, A.D., Lane, T.E., Fitchen, J.H., Buchmeier, M.J., Beachy, R.N., 1999. Protective immunity against murine hepatitis virus (MHV) induced by intranasal or subcutaneous administration of hybrids of tobacco mosaic virus that carries an MHV epitope. Proc. Natl. Acad. Sci. U. S. A. 96 (14), 7774–7779.

Ksiazek, T.G., Erdman, D., Goldsmith, C.S., Zaki, S.R., Peret, T., Emery, S., Tong, S., Urbani, C., Comer, J.A., Lim, W., Rollin, P.E., Dowell, S.F., Ling, A.E., Humphrey, C.D., Shieh, W.J., Guarner, J., Paddock, C.D., Rota, P., Fields, B., DeRisi, J., Yang, J.Y., Cox, N., Hughes, J.M., LeDuc, J.W., Bellini, W.J., Anderson, L.J., 2003. A novel coronavirus associated with severe acute respiratory syndrome. N. Engl. J. Med. 348 (20), 953–966.

Kubo, H., Takase-Yoden, S., Taguchi, F., 1993. Neutralization and fusion inhibition activities of monoclonal antibodies specific for the S1 subunit of the spike protein of neurovirulent murine coronavirus JHMV c1-2 variant. J. Gen. Virol. 74 (Pt 7), 1421–1425.

Kubo, H., Yamada, Y.K., Taguchi, F., 1994. Localization of neutralizing epitopes and the receptor-binding site within the amino-terminal 330 amino acids of the murine coronavirus spike protein. J. Virol. 68 (9), 5403–5410.

Lai, M.M.C., Holmes, K.V., 2001. Coronviridae: the viruses and their replication, 4th ed. Knipe, D.M., Howley, P.M. (Eds.), Fields Virology (vol. 1. Lippincott-Raven, Philadelphia, pp. 1163–1184 (2 vols).

Lau, L.T., Fung, Y.W., Wong, F.P., Lin, S.S., Wang, C.R., Li, H.L., Dillon, N., Collins, R.A., Tam, J.S., Chan, P.K., Wang, C.G., Yu, A.C., 2003. A real-time PCR for SARS-coronavirus incorporating target gene pre-amplification. Biochem. Biophys. Res. Commun. 312 (4), 1290–1296.

Leparc-Goffart, I., Hingley, S.T., Jiang, X., Chua, M.M., Lavi, E., Weiss, S.R., 1998. The C12 mutant of MHV-A59 is very weakly demyelinating and has five amino acid substitutions restricted to the spike and replicase genes. Adv. Exp. Med. Biol. 440, 627–633.

Li, D., Cavanagh, D., 1990. Role of pH in syncytium induction and genome uncoating of avian infectious bronchitis coronavirus (IBV). Adv. Exp. Med. Biol. 276, 33–36.

Li, D., Cavanagh, D., 1992. Coronavirus IBV-induced membrane fusion occurs at near-neutral pH. Arch. Virol. 122 (3–4), 307–316.

Li, W., Moore, M.J., Vasilieva, N., Sui, J., Wong, S.K., Berne, M.A., Somasundaran, M., Sullivan, J.L., Luzuriaga, K., Greenough, T.C., Choe, H., Farzan, M., 2003. Angiotensin-converting enzyme 2 is a functional receptor for the SARS coronavirus. Nature 426 (6965), 450–454.

Marra, M.A., Jones, S.J., Astell, C.R., Holt, R.A., Brooks-Wilson, A., Butterfield, Y.S., Khattra, J., Asano, J.K., Barber, S.A., Chan, S.Y., Cloutier, A., Coughlin, S.M., Freeman, D., Girn, N., Griffith, O.L., Leach, S.R., Mayo, M., McDonald, H., Montgomery, S.B., Pandoh, P.K., Petrescu, A.S., Robertson, A.G., Schein, J.E., Siddiqui, A., Smailus, D.E., Stott, J.M., Yang, G.S., Plummer, F., Andonov, A., Artsob, N., Bastien, N., Bernard, K., Booth, T.F., Bowness, D., Czub, M., Drebot, M., Fernando, L., Flick, R., Garbutt, M., Gray, M., Grolla, A., Jones, S., Feldmann, H., Meyers, A., Kabani, A., Li, Y., Normand, S., Stroher, U., Tipples, G.A., Tyler, S., Vogrig, R.,Ward, Vogrig, D., Watson, B., Brunham, R.C., Krajden, M., Petric, M., Skowronski, D.M., Upton, C., Roper, R.L., 2003. The genome sequence of the SARS-associated coronavirus. Science 300 (5624), 1399–1404.

Martina, B.E., Haagmans, B.L., Kuiken, T., Fouchier, R.A., Rimmelzwaan, Fouchier, G.F., Van Amerongen, G., Peiris, J.S., Lim, W., Osterhaus, A.D., 2003. Virology: SARS virus infection of cats and ferrets. Nature 425 (6961), 915.

Moss, B., Elroy-Stein, O., Mizukami, T., Alexander, W.A., Fuerst, T.R., 1990. New mammalian expression vectors. Nature 348 (6296), 91–92.

Nash, T.C., Buchmeier, M.J., 1997. Entry of mouse hepatitis virus into cells by endosomal and nonendosomal pathways. Virology 233 (1), 1–8.

Ng, E.K., Hui, D.S., Chan, K.C., Hung, E.C., Chiu, R.W., Lee, N., Wu, A., Chim, S.S., Tong, Y.K., Sung, J.J., Tam, J.S., Lo, Y.M., 2003. Quantitative analysis and prognostic implication of SARS coronavirus RNA in the plasma and serum of patients with severe acute respiratory syndrome. Clin. Chem. 49 (12), 1976–1980.

Ogert, R.A., Lee, M.K., Ross, W., Buckler-White, A., Martin, M.A., Cho, M.W., 2001. N-linked glycosylation sites adjacent to and within the V1/V2 and the V3 loops of dualtropic human immunodeficiency virus type 1 isolate DH12 gp120 affect coreceptor usage and cellular tropism. J. Virol. 75 (13), 5998–6006.

Payne, H.R., Storz, J., Henk, W.G., 1990. Initial events in bovine coronavirus infection: analysis through immunogold probes and lysosomotropic inhibitors. Arch. Virol. 114 (3–4), 175–189.

Peiris, J.S., Lai, S.T., Poon, L.L., Guan, Y., Yam, L.Y., Lim, W., Nicholls, J., Yee, W.K., Yan, W.W., Cheung, M.T., Cheng, V.C., Chan, K.H., Tsang, D.N., Yung, R.W., Ng, T.K., Yuen, K.Y., 2003. Coronavirus as a possible cause of severe acute respiratory syndrome. Lancet 361 (9366), 1319–1325.

Picard-Maureau, M., Jarmy, G., Berg, A., Rethwilm, A., Lindemann, D., 2003. Foamy virus envelope glycoprotein-mediated entry involves a pH-dependent fusion process. J. Virol. 77 (8), 4722–4730.

Poon, L.L., Chan, K.H., Wong, O.K., Yam, W.C., Yuen, K.Y., Guan, Y., Lo, Y.M., Peiris, J.S., 2003aa. Early diagnosis of SARS Coronavirus infection by real time RT-PCR. J. Clin. Virol. 28 (3), 233–238.

Poon, L.L., Wong, O.K., Chan, K.H., Luk, W., Yuen, K.Y., Peiris, J.S., Guan, Y., 2003bb. Rapid diagnosis of a coronavirus associated with severe acute respiratory syndrome (SARS). Clin. Chem. 49 (6 Pt 1), 953–955.

Poutanen, S.M., Low, D.E., Henry, B., Finkelstein, S., Rose, D., Green, K., Tellier, R., Draker, R., Adachi, D., Ayers, M., Chan, A.K., Skowronski, D.M., Salit, I., Simor, A.E., Slutsky, A.S., Doyle, P.W., Krajden, M., Petric, M., Brunham, R.C., McGeer, A.J., 2003. Identification of severe acute respiratory syndrome in Canada. N. Engl. J. Med. 348 (20), 995–2005.

Reitter, J.N., Means, R.E., Desrosiers, R.C., 1998. A role for carbohydrates in immune evasion in AIDS. Nat. Med. 4 (6), 679–684.

Rota, P.A., Oberste, M.S., Monroe, S.S., Nix, W.A., Campagnoli, R., Icenogle, J.P., Penaranda, S., Bankamp, B., Maher, K., Chen, M.H., Tong, S., Tamin, A., Lowe, L., Frace, M., DeRisi, J.L., Chen, Q., Wang, D., Erdman, D.D., Peret, T.C., Burns, C., Ksiazek, T.G., Rollin, P.E., Sanchez, A., Liffick, S., Holloway, B., Limor, J., McCaustland, K., Olsen-Rasmussen, M., Fouchier, R., Gunther, S., Osterhaus, A.D., Drosten, C., Pallansch, M.A., Anderson, L.J., Bellini, W.J., 2003. Characterization of a novel coronavirus associated with severe acute respiratory syndrome. Science 300 (5624), 1394–1399.

Sanchez, C.M., Izeta, A., Sanchez-Morgado, J.M., Alonso, S., Sola, I., Balasch, M., Plana-Duran, J., Enjuanes, L., 1999. Targeted recombination demonstrates that the spike gene of transmissible gastroenteritis coronavirus is a determinant of its enteric tropism and virulence. J. Virol. 73 (9), 7607–7618.

Schnierle, B.S.S.J., Bosch, V., Nocken, F., Merget-Millitzer, H., Engelstadter, M., Kurth, R., Groner, B., Cichutek, K., 1997. Pseudotyping of murine leukemia virus with the envelope glycoproteins of HIV generates a retroviral vector with specificity of infection for CD4-expressing cells. Proc. Natl. Acad. Sci. U. S. A. 94 (16), 8640–8645.

Simmons, G., Reeves, J.D., Rennekamp, A.J., Amberg, S.M., Piefer, A.J., Bates, P., 2004. Characterization of severe acute respiratory syndrome-associated coronavirus (SARS-CoV) spike glycoprotein-mediated viral entry. Proc. Natl. Acad. Sci. U. S .A. 101 (12), 4240–4245.

Snijder, E.J., Bredenbeek, P.J., Dobbe, J.C., Thiel, V., Ziebuhr, J., Poon, L.L., Guan, Y., Rozanov, M., Spaan, W.J., Gorbalenya, A.E., 2003. Unique and conserved features of genome and proteome of SARS-coronavirus, an early split-off from the coronavirus group 2 lineage. J. Mol. Biol. 331 (5), 991–1004.

Takase-Yoden, S., Kikuchi, T., Siddell, S.G., Taguchi, F., 1991. Localization of major neutralizing epitopes on the S1 polypeptide of the murine coronavirus peplomer glycoprotein. Virus Res. 18 (2–3), 99–107.

Tang, P., Louie, M., Richardson, S.E., Smieja, M., Simor, A.E., Jamieson, F., Fearon, M., Poutanen, S.M., Mazzulli, T., Tellier, R., Mahony, J., Loeb, M., Petrich, A., Chernesky, M., McGeer, A., Low, D.E., Phillips, E., Jones, S., Bastien, N., Li, Y., Dick, D., Grolla, A., Fernando, L., Booth, T.F., Henry, B., Rachlis, A.R., Matukas, L.M., Rose, D.B., Lovinsky, R., Walmsley, S., Gold, W.L., Krajden, S., 2004. Interpretation of diagnostic laboratory tests for severe acute respiratory syndrome: the Toronto experience. CMAJ 170 (1), 47–54.

Tsai, C.W., Chang, S.C., Chang, M.F., 1999. A 12-amino acid stretch in the hypervariable region of the spike protein S1 subunit is critical for cell fusion activity of mouse hepatitis virus. J. Biol. Chem. 274 (37), 26085–26090.

Wang, J., Wen, J., Li, J., Yin, J., Zhu, Q., Wang, H., Yang, Y., Qin, E., You, B., Li, W., Li, X., Huang, S., Yang, R., Zhang, X., Yang, L., Zhang, T., Yin, Y., Cui, X., Tang, X., Wang, L., He, B., Ma, L., Lei, T., Zeng, C., Fang, J., Yu, J., Yang, H., West, M.B., Bhatnagar, A., Lu, Y., Xu, N., Liu, S., 2003. Assessment of immunoreactive synthetic peptides from the structural proteins of severe acute respiratory syndrome coronavirus. Clin. Chem. 49 (12), 1979–1980.

WHO, 2003. Summary of probable SARS cases with onset of illness from 1 November 2002 to 31 July 2003 World Health Organization. http://www.who.int/csr/sars/country/table2003_09_23/en/.

Xiao, X., Chakraborti, S., Dimitrov, A.S., Gramatikoff, K., Dimitrov, D.S., 2003. The SARS-CoV S glycoprotein: expression and functional characterization. Biochem. Biophys. Res. Commun. 312 (4), 1159–1164.

Yam, W.C., Chan, K.H., Poon, L.L., Guan, Y., Yuen, K.Y., Seto, W.H., Peiris, J.S., 2003. Evaluation of reverse transcription-PCR assays for rapid diagnosis of severe acute respiratory syndrome associated with a novel coronavirus. J. Clin. Microbiol. 41 (10), 4521–4524.

Yamada, Y.K., Takimoto, K., Yabe, M., Taguchi, F., 1998. Requirement of proteolytic cleavage of the murine coronavirus MHV-2 spike protein for fusion activity. Adv. Exp. Med. Biol. 440, 89–93.